

An environmentally friendly indigo dyeing process using iron (II) gluconate as a reducing agent

Maha Abdelileh^{1,2*}, Manel Ben Ticha³, Nizar Meksi^{1,2}, Hatem Dhaouadi¹

¹ *University of Monastir, Faculty of Sciences of Monastir, Research Laboratory of Environmental Chemistry and Clean Processes, 5000 Monastir, Tunisia.*

² *University of Monastir, National Engineering School of Monastir, Department of Textile, 5000 Monastir, Tunisia.*

³ *Department of Early Childhood, University College of Turabah, Taif University, Taif 21944, Saudi Arabia*

<https://doi.org/10.2298/CICEQ240106022A>

Received 6.1.2024.

Revised 3.6.2024.

Accepted 10.6.2024.

* Corresponding author. Email: maha.abdelileh@gmail.com.

Address: Research Laboratory of Environmental Chemistry and Clean Processes, Faculty of Sciences of Monastir - 5000 Monastir, TUNISIA

Telephone number : (+216) 94347944

ABSTRACT

This research paper aims to replace the ecologically harmful sodium dithionite traditionally used in the indigo dyeing process with the iron (II) gluconate reducing agent. The density functional theory (DFT) method using B3LYP 6- 311 G basis set was used to determine the optimized structures of iron (II) gluconate and indigo. The highest occupied molecular orbital (HOMO) energy and the lowest unoccupied molecular orbital (LUMO) energy were calculated, and the electronic properties dependent on HOMO-LUMO energies were determined. Furthermore, an ecological dyeing process using this reducing agent was studied. The influences of alkalinity, reduction temperature, and iron (II) gluconate concentration on the fulfilment of the dyeing process were inspected by measuring the obtained redox potential and the color strength of the dyed samples. A full factorial experiment was performed for statistical analysis and optimization of the dyeing process. The results revealed that the developed method is highly effective and capable of generating redox potential and dyeing quality comparable to those obtained with the conventional process employing sodium dithionite. Finally, the substitution of sodium dithionite by iron (II) gluconate reduced the wastewater load generated by the conventional dyeing process.

KEYWORDS

Indigo dyeing; density functional theory; ecological process; iron (II) gluconate; process optimization.

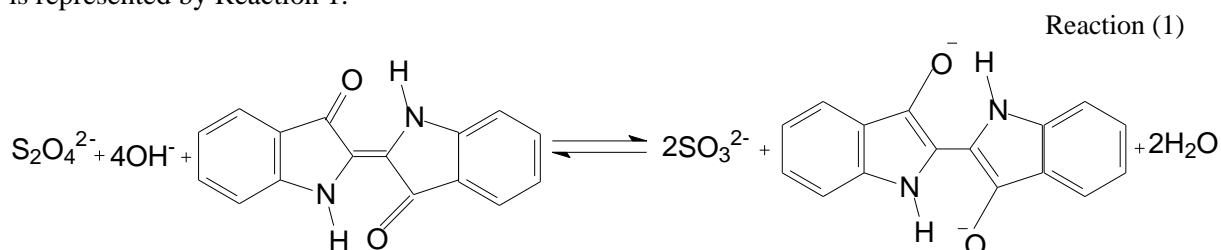
Highlights :

- An ecological indigo dyeing process using iron (II) gluconate as a reducing agent was studied.
- Iron (II) gluconate molecule is very stable with high hardness, and a large energy gap
- A comparable dyeing quality to that of the conventional process has been achieved.
- Cleaner wastewater was obtained by this dyeing process.

INTRODUCTION

With annual sales of over 5 billion blue jeans worldwide, the production of denim fabric is considered one of the most important sectors of the clothing industry [1]. As economic progress and living standards improve, the importance of indigo, the dye used in denim production, continues to grow within the dyeing sector for blue jeans [2].

In the continuous dyeing process, this initially insoluble dye needs to be converted into its leuco-soluble form, which exhibits a low affinity for cellulosic fibers. During dyeing, cotton yarns are submerged in a dye bath containing the reduced form of indigo (leuco indigo), squeezed, and subsequently exposed to air, to convert the leuco dye back to its original insoluble form. To achieve the necessary dye fixation, the immersion and oxidation steps must be repeated multiple times. Nowadays, most indigo dyeing processes rely on the utilization of sodium dithionite ($\text{Na}_2\text{S}_2\text{O}_4$) as a reducing agent to obtain the soluble leuco form of the dye. The reduction reaction of indigo with conventional sodium dithionite in an alkaline medium is represented by Reaction 1.



Nevertheless, the use of this reductant has been attacked for the formation of by-products such as sulfides, sulfites, sulfates, thiosulfates, and toxic sulfur. These by-products have a hazardous impact on the environment when released into sewage due to their toxicity. Furthermore, the release of large amounts of sodium dithionite into wastewater increases the wastewater treatment burden [3]. Therefore, many initiatives have been developed to substitute sodium dithionite with more environmentally friendly alternatives, such as the electrochemical reduction of indigo [4]. This method uses a regenerable redox system in the dye bath, which is constantly regenerated by cathodic reduction [5,6].

Several mediator solutions, including anthraquinonoid compounds [7] and iron (II) complexes with various ligands such as iron(II)-sodium gluconate-Abal B [1] and iron-triethanolamine-calcium gluconate [8] have been used to reduce indigo. These mediator solutions have demonstrated comparable dyeing performance to the standard indigo dyeing process utilizing sodium dithionite. Furthermore, Changhai et al.'s patent describes an indirect electrochemical reduction using gluconic acid and iron triethanolamine as a regenerable redox system to generate a synergistic effect [9]. This method enhances current efficiency, leading to a significant reduction in energy consumption, thus making it cost-effective. Also, the utilization of a divalent copper ion complex combined with electrochemical technology for reducing indigo using sodium borohydride at room temperature has been investigated by Xiaoyan and his team [10]. Through the optimization of experimental conditions, they achieved a redox potential of -968mV and a K/S value of 11.92, comparable to that of the conventional reduction process with sodium dithionite. Indirect electrochemical reduction technology not only reduces chemical usage but also enables the

control of dye reduction conditions using electrochemical techniques. While direct recycling of the mediator solution and water is possible, it comes with significant energy demands and necessitates a sizable electrode surface. Moreover, there is an additional expense associated with mediator filtration.

Besides, the use of organic reductants as greener alternatives to sodium dithionite such as sodium borohydride [11,12] and α -hydroxyketones [13] are widely used. These reducing agents can make the grades of efficiency and biodegradability. Ferrous salts have been extensively used to reduce indigo. Indeed the use of iron (II) sulfate complexed with various ligands such as tartaric, citric, and gluconic acids for indigo reduction and dyeing in the presence of NaOH was studied [14-16]. This method enhances the solubility of iron (II) hydroxide in the dye bath responsible for the indigo reduction and gives an acceptable dyeing quality and cleaner effluents. Subsequent removal of gluconic acid is achieved by neutralization with a small amount of alkali in the wastewater tank.

This paper reports the application of iron (II) gluconate for indigo reduction and dyeing. This ferrous compound is generally used as a food additive and dietary supplement. The ionization energy, electron affinity and global reactivity descriptors of iron (II) gluconate and indigo were calculated using DFT method. Similarly the nucleophilic and electrophilic sites of iron (II) gluconate were determined by molecular electrostatic potential (MEP). An environmentally friendly process was developed for dyeing cotton with indigo using iron (II) gluconate as a reducing agent. The influence of experimental parameters (sodium hydroxide concentration, reduction temperature, and iron (II) gluconate concentration) on redox potential and dyeing performance was studied. During the dyeing process, this reducing agent is converted after aeration to a ferric compound that acts as a flocculant and will be removed during wastewater treatment [16]. For statistical analysis, a full factorial experiment was performed to obtain the optimal experimental conditions for indigo reduction. The residual dye bath of the process using ferrous gluconate as reducing agent was evaluated and compared to the process using sodium dithionite.

EXPERIMENTAL

Chemicals and Materials

The chemicals used were of analytical grade: Sodium hydroxide (NaOH, $\geq 99\%$, Loba Chemie, Germany), iron (II) gluconate dihydrate ($C_{12}H_{22}FeO_{14}$, Sigma-Aldrich, USA), sodium dithionite ($Na_2S_2O_4$, BASF, Germany), ammonium iron (II) sulfate ($(NH_4)Fe(SO_4)_2(H_2O)_6 \geq 99\%$, Sigma-Aldrich, USA), potassium dichromate ($K_2Cr_2O_7 \geq 99\%$, Sigma-Aldrich, USA), mercury(II) sulfate ($HgSO_4$, Chemsolute, Germany), sulfuric acid ($H_2SO_4 \geq 95\%$, Scharlau, Spain), silver sulfate ($Ag_2SO_4 \geq 99\%$, Sigma-Aldrich, USA).

Indigo powder ($C_{16}H_{10}N_2O_2$, Benzema, Switzerland) was used for dyeing cotton samples. For dyeing experiments, a bleached cotton fabric (100% cotton) was used with the following specifications: plain weave, mass per area 173 g/m², warp count of 25 yarns/cm, and weft count of 31 yarns/cm.

Computational details

The DFT calculations were carried out using Gaussian program package 09, while Gauss View 5 was used for visualization of the structure and simulation of the vibrational spectra. In this study B3LYP 6-311 G basis set was employed to obtain the optimized structures with minimum energy of iron (II) gluconate and indigo. The ionization Energy (IE), electron affinity (EA) and global reactivity descriptors such as chemical potential, hardness, softness, electronegativity and electrophilicity index of iron (II) gluconate and indigo molecules have been evaluated from highest occupied molecular orbital (HOMO) and lowest unoccupied molecular orbital (LUMO) frontier molecular (FMO) energy values. The global reactivity descriptors using Koopman's theorem [17] are given by the following equations:

$$\text{The chemical potential : } \mu = \frac{-(IE+EA)}{2} \quad (1)$$

$$\text{The hardness : } \eta = \frac{(IE-EA)}{2} \quad (2)$$

$$\text{The softness : } s = \frac{1}{2\eta} \quad (3)$$

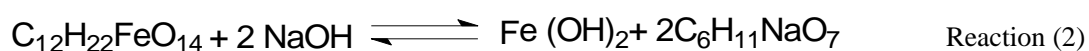
$$\text{The electronegativity : } \chi = \frac{(IE+EA)}{2} \quad (4)$$

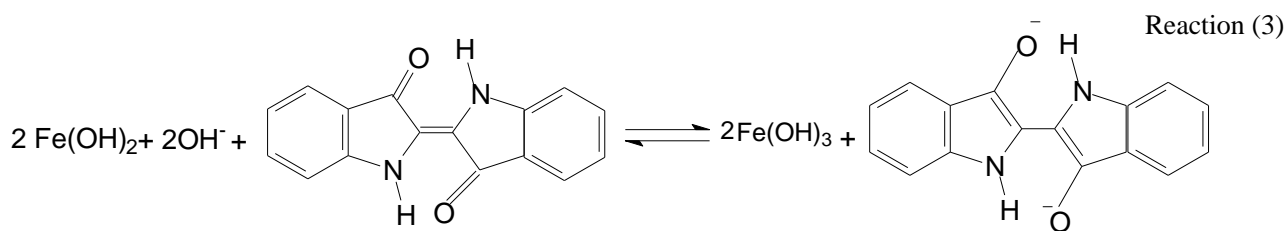
$$\text{Global electrophilicity index : } \omega = \frac{\mu^2}{2\eta} \quad (5)$$

where the ionization energy $IE = -EHOMO$ and the electron affinity $EA = -ELOMO$

Indigo reduction processes

A solution containing 2 g·L⁻¹ of indigo, sodium hydroxide ranging from 5 to 30 g·L⁻¹, and iron (II) gluconate ranging from 2 to 25 g·L⁻¹, was heated to a temperature between 50°C and 90°C for a duration of 2 hours. The indigo reduction was executed in AHIBA dyeing machine, and redox potential measurements were performed at the end of the process using a pH meter (pHM210) equipped with a platinum electrode and a reference electrode (Ag/AgCl, 3KCl). Iron (II) gluconate, in an alkaline medium, generates iron (II) hydroxide which is a reducing agent known for its ability to reduce vat dyes, especially indigo [18] (Reaction 2). The reduction reaction of indigo with iron(II) gluconate is represented by Reaction 3. The reduced bath was then used for dyeing experiments using the (6dip-6nip) method, elucidated thoroughly in the subsequent section.





To compare the dyeing results achieved with iron (II) gluconate as a reducing agent with those of conventional methods, a series of tests employing sodium dithionite as a reducing agent were conducted. These tests adhered to the guidelines of the traditional process used at an industrial scale. Typically, the dye bath contains $2 \text{ g}\cdot\text{L}^{-1}$ of indigo, $4\text{g}\cdot\text{L}^{-1}$ of sodium hydroxide, and $4 \text{ g}\cdot\text{L}^{-1}$ of sodium dithionite, maintained at a temperature of 50°C for 2 hours [19].

Dyeing process

Cotton samples were dyed by impregnation. After dipping the samples in the dye bath for 1 min, they were exposed to air for approximately 2 min, to complete a cycle (1 dip-1 nip). This step was repeated 6 times. Afterward, the samples were cold rinsed and dried at ambient temperature.

Color strength measurement

The dyeings were assessed by measuring the color strength (K/S) at 660 nm using a spectraflash 600+ spectrophotometer (Datacolor international, USA, illuminant : D 65, geometry: d/10°). The presented results were calculated as the mean of three values. The color strength value (K/S) was calculated according to the following equation [20] :

$$\frac{K}{S} = \frac{(1-R)^2}{2R} - \frac{(1-R_0)^2}{2R_0} \quad (6)$$

where R is the decimal fraction of the reflectance of dyed sample, R_0 is the decimal fraction of the reflectance of undyed sample, K is the absorption coefficient, and S is the scattering coefficient.

Bath exhaustion measurement

A volume of 1 mL was extracted from the dyeing bath. Subsequently, it was oxidised in 100 mL of distilled water under vigorous stirring for a few minutes. The absorbance of the oxidized leuco-indigo bath before and after dyeing was measured using a UV-visible spectrophotometer (Shimadzu, Japan). The bath exhaustion percentage (E %) was calculated using the following equation [21] :

$$E(\%) = \frac{(A_0 - A_r)}{A_0} \times 100 \quad (7)$$

Where, A_0 and A_r represent the absorbance of the oxidized leuco-indigo bath before and after dyeing, respectively.

Evaluation of dyeing fastnesses

The dyeing fastness to washing, rubbing, and light of the various samples dyed with indigo was evaluated according to the following ISO standards respectively: ISO 105- C06, ISO 105- X12, and ISO 105-B02.

Environmental evaluation of the residual dyeing baths

The residual dyeing bath was assessed by measuring the chemical oxygen demand (COD), the biological oxygen demand (BOD), and the pH of the dyeing bath. The (COD) in the dyebath after dyeing was assessed conforming to the method described by Harrelkas [22]. This method involves the chemical oxidation of the reducing substances in water using an excess of potassium dichromate $K_2Cr_2O_7$ in a sulfuric medium. The (COD) measurement implies titrating the excess potassium dichromate with a reducing agent, ammonium iron(II) sulfate. Initially, 2.5mL of the sample under analysis was introduced into a digestion tube following agitation. Subsequently, 1.5 mL of digestion solution (consisting of 12.25 $g \cdot L^{-1}$ potassium dichromate dried for 2 hours at 105°C, 33.3 $g \cdot L^{-1}$ mercury sulfate, and 167 mL sulfuric acid in 1L distilled water) and 3.5mL catalyst solution (8.8 $g \cdot L^{-1}$ silver sulfate in 1L sulfuric acid) are added to the digestion tube. The sealed tubes were then subjected to a temperature of 148°C in a reactor for a duration of 2 hours. Following cooling, the contents of the tubes were poured into a 50mL Erlenmeyer flask and the volume was made up to 25 mL. A few drops of ferroin (color indicator) were added, and titration was carried out using 0.12M Mohr's salt solution. Additionally, a blank was prepared using 2.5mL of distilled water following the same procedure. The COD of the analyzed samples is expressed in $mg O_2/L$ and it is equal to:

$$COD = 8000 \times CX \frac{(VB-VE)}{V} \quad (8)$$

Where VB: is the volume of Mohr's salt poured to determine the blank solution; VE: is the volume of Mohr's Salt poured to determine the sample, $C=0.12M$, and V: is the volume of the sample [23].

To determine the biological oxygen demand (BOD)₅, dissolved oxygen (DO) was measured before and after 5 days of culture in a BOD incubator at 26 °C. Oxygen consumption was followed for 5 days. This parameter is transformed by the atmospheric pressure drop. The (BOD)₅ is thus equal to:

$$(BOD)_5 = (P_0 - P_5) \times F \quad (9)$$

P₀: is the O₂ concentration in the solution at the beginning of the assay; P₅ is the O₂ concentration in the solution at the end of the assay (after 5 days); and F=10 is the dilution factor.

Statistical analysis and process optimization

A full-factorial experimental design with three factors and three levels was implemented to model and optimize the dyeing process. This experimental design allows us to study the influence of the experimental parameters (iron (II) gluconate concentration, reduction temperature, and alkali concentration) and to optimize the dyeing process. The input parameters and their levels are represented in Table S1. All reduction experiments were performed using 2 $g \cdot L^{-1}$ of indigo for 2h. Analysis of variance (ANOVA) was performed, and the P-value was used to demonstrate the significance of each parameter [24]. The analyzed

responses are the redox potential and color strength (K/S) of the dyed samples. The experimental design, along with different experiments and responses, is displayed in Table S2.

-Table S1 -

-Table S2-

RESULTS AND DISCUSSION

DFT study of iron(II) gluconate and indigo

Prediction of global reactivity descriptors for iron(II) gluconate and indigo

According to the frontier molecular orbital theory (FMO) of chemical reactivity, the transition of an electron occurs through the interaction between the highest occupied molecular orbital (HOMO) and the lowest unoccupied molecular orbital (LUMO) of the reacting species [25]. The HOMO and LUMO energies of both iron (II) gluconate and indigo were calculated by the functional/standard basis set B3LYP/6-311G. Global reactivity descriptors of iron (II) gluconate and indigo such as ionization energy (IE), electron affinity (EA), electronegativity (χ), chemical hardness (η), chemical softness (S), chemical potential values (μ) and electrophilicity index (ω) were determined based on gas-phase optimization. These numerical parameters, which are mainly calculated from HOMO and LUMO energies, are summarized in Table 1.

-Table 1-

E_{HOMO} , a quantum chemical parameter, is commonly linked to the electron-donating capability of a molecule. The high value E_{HOMO} value suggests that the molecule is more inclined to donate electrons to a suitable acceptor molecule of low empty molecular orbital [26]. Referring to Table 1, it can be noted that iron(II) gluconate has a higher E_{HOMO} absolute value compared to the E_{LUMO} absolute value of indigo indicating a favorable energy difference for electron transfer from iron(II) gluconate to indigo. This result highlights the capacity of iron(II) gluconate to donate electrons to indigo.

The global properties which are very useful in evaluating the molecular stability and reactivity are hardness and softness. A molecule is considered hard when it possesses a large energy gap, whereas a soft molecule is characterized by a smaller energy gap [27]. The molecule iron (II) gluconate has a very high hardness of 2.23 (ev) and a very low softness of 0.224 (ev) due to the high energy gap. Consequently the molecule is demonstrated to be extremely stable, displaying low chemical reactivity and high kinetic stability.

-Figure 1 -

Local chemical activity calculations: Molecular Electrostatic Potential (MEP)

Electrophilic nature, nucleophilic reactions, hydrogen bond interactions can be elucidated through the molecular electrostatic potential, which is associated with electron density. Molecular electrostatic

potential surfaces are visually depicted using color codes, where red signifies the most negative regions indicative of electrophilic reactions. Conversely, blue and green indicate the most positive regions, representing nucleophilic dominant regions [28- 30]. The total electron density surface of iron (II) gluconate is given in Figure 2. This figure illustrates that in iron(II) gluconate, most positive charges are concentrated around the iron atom, defining potential nucleophilic reactions, while the most negative charges are localized around the oxygen atoms. These regions indicate a higher electron density, suggesting that they are more likely to donate electrons. Thus, iron(II) gluconate may act as a potential reducing agent for indigo.

-Figure 2 -

Study of the dyeing process

Effect of the reduction temperature

The evolution of the redox potential and color strength of the dyed samples as a function of reduction temperature is presented in Figure 3(a). This figure, shows that increasing the temperature from 50 to 75 °C improves the reducing power and color strength. This result can be attributed to the fact that increasing the temperature promotes molecular agitation and leads to a better reduction of the dye. Therefore, a higher concentration of leuco-indigo is adsorbed on the fabric. Above this temperature, a slight decrease in the reducing power and color strength is observed. This result could be explained by the fact that higher temperatures may reduce the yield of indigo reduction while simultaneously increasing the hydrolysis reaction, which can negatively impact the dyeing process [11].

Effect of iron (II) gluconate concentration

The concentration of iron (II) gluconate varied from 2 to 25 g·L⁻¹, and the evolution of redox potential and color strength were studied. As shown in Figure 3 (b), for concentrations below 18 g·L⁻¹, the redox potential gradually decreases, reaching a minimum value of -745 mV and color strength increases to a maximum value of 19.2. This result can be attributed to the fact that increasing the leuco-indigo concentration leads to an increase in the absorption into the fiber. While exceeding a concentration of 18 g·L⁻¹, the redox potential and color strength remained almost constant, indicating that the maximum concentration of leuco-indigo was probably reached.

Effect of sodium hydroxide concentration

The influence of sodium hydroxide concentration on the redox potential and color strength of the dyed samples is presented in Figure 3 (c). The obtained curves shows that at a sodium hydroxide concentration of 20 g·L⁻¹, the redox potential decreases until it reaches a value of -671 mV and color strength increases to reach a value of 13.5. This result can be accounted for the fact that raising the sodium hydroxide

concentration in the medium promotes the leuco-indigo formation, generates more negative redox potential values, and increases the dye uptake by the fibers. Above a concentration of $20 \text{ g}\cdot\text{L}^{-1}$, an increase in the redox potential and a drop in the color strength are observed. This result is probably due to an over-reduction of indigo. Therefore, a sodium hydroxide concentration between 15 and $20 \text{ g}\cdot\text{L}^{-1}$ is sufficient to achieve the optimum dyeing quality.

-Figure 3 –

Optimization of the dyeing process

Statistical analysis and optimization of the experimental data were carried out using the software (Minitab Ver. 17.0, USA). The determination of the regression model, the main effects, and the interactions between factors were performed.

Establishment of models

An analysis of the regression equation determines the relationship between the responses and the various factors. By taking into account the detected effects (linear, quadratic) and interactions, this feature allows the adjustment of the model. The experimental analysis leads to the regression coefficients for the redox potential and color strength (Tables S3 and S4). The assessment was based on the P-value (Fisher coefficient) of each parameter. This coefficient is used to identify the significance of each parameter. In general, a factor is considered significant if it has a P value <0.05 . The quadratic analysis of the two responses leads to the following regression equations

$$\text{PR} = -422.674 - 4.0313 \text{ S}(\text{g}\cdot\text{L}^{-1}) - 7.13304 \text{ Red}(\text{g}\cdot\text{L}^{-1}) + 0.1564 \text{ S}^2(\text{g}\cdot\text{L}^{-1}) - 0.2456 \text{ S}(\text{g}\cdot\text{L}^{-1}) \times \text{Red}(\text{g}\cdot\text{L}^{-1}) \quad (11)$$

with $R^2 = 93.4\%$

$$\text{K/S} = -34.3275 + 0.7764 \text{ S}(\text{g}\cdot\text{L}^{-1}) + 3.1859 \text{ Red}(\text{g}\cdot\text{L}^{-1}) - 0.0258 \text{ S}^2(\text{g}\cdot\text{L}^{-1}) \quad \text{With } R^2 = 94.1\% \quad (12)$$

For both redox potential and color strength, high determination coefficients R^2 were obtained. Therefore the models correctly estimated the geometrical deviations according to the three selected factors and their interactions.

-Table S3-

-Table S4-

Principal effects of the experimental parameters

The influence of the factors on the color strength and redox potential was determined using main effect diagrams (Figure 4(a)). Based on this figure, it can be noted that the reducing agent concentration and the sodium hydroxide concentration have the highest effect on both the redox potential and color strength. It can also be noted that reduction temperature has a less important effect on both responses. The optimal reduction temperature is 75° C. If the temperature exceeds this level, the color strength decreases rapidly.

Analysis of interaction graphs

Figure 4(b) represents the interaction plots between the studied parameters (iron (II) gluconate concentration, reduction temperature, and sodium hydroxide concentration). This figure shows that there is no interaction between the different studied factors for color strength. The plot for the redox potential shows an interaction between the iron (II) gluconate concentration and the alkali concentration. This relation can be interpreted by the fact that the indigo reduction requires the formation of a certain amount of iron (II) hydroxide, resulting from the reaction of sodium hydroxide with iron (II) gluconate. In addition, this graph indicates that there is no interaction between the reducing agent concentration and temperature, and between the alkali concentration and temperature.

Contour plots analysis

Contour graphs give an idea about the zones that can maximize the response value when combining two input parameters. Contour plots of color strength and redox potential are given in Figure 4(c). This figure reveals the regions of maximum color strength ($K/S > 15$). These areas are shown in dark green. As shown in figure 4(c), the lowest redox potential values (between -660 mV and -680 mV) were obtained at high reducing agent and sodium hydroxide concentrations.

-Figure 4-

Optimization of the reduction process

The optimum reduction conditions are shown in Table 2. To confirm the theoretical value reported by the Minitab software, the dyeing experiment under these optimum conditions was repeated three times. An average value of 20.1 ± 0.36 was obtained. Hence, the validation of the optimal conditions.

-Table 2-

Evaluation of the dyeing performance

To evaluate the potential use of the optimized process using iron (II) gluconate as a replacement for the conventional process using sodium dithionite, a comparative analysis involving the measurement of redox

potential, color strength of the indigo dyed samples, dyeing fastness and bath exhaustion percentage was conducted. The results are shown in Table 3, with each value in the table representing the mean value of three experiments. This table reveals that iron (II) gluconate exhibits a redox potential slightly higher than that obtained with sodium dithionite. Moreover, despite its higher redox potential, the process using iron (II) gluconate as a reducing agent demonstrates superior performance in dyeing processes compared to the reference dyeings with sodium dithionite. Notably, it yields higher color strength, exhaustion percentage and dyeing fastness indicating its effectiveness in the dyeing process. This result could be explained by the presence of iron (II) in the dye bath, which acts as a mordant that establishes chemical bonds between the fiber and the dye via the metal, subsequently darkening the shades and improving dyeing fastness.

-Table 3-

Environmental assessment of residual dye baths

The residual bath of the indigo dyeing process using iron (II) gluconate as a reductant was evaluated. Indigo reduction was carried out under optimum conditions. The effluent quality was compared to that of the standard process using sodium dithionite. Table 4 summarizes the parameters measured for the residual bath in both processes. The obtained results show that the effluent from the conventional process presents a COD/BOD₅ ratio of about 6, which indicates that this effluent is highly polluting and hardly biodegradable. On the other hand, the substitution of sodium dithionite by iron (II) gluconate allows the reduction of this ratio and therefore reduces the wastewater pollution generated by the classical process. These effluents will then be subjected to wastewater treatment. For the case of reduced indigo by iron (II) gluconate, the free iron(II) hydroxide is transformed by oxidation into Fe(OH)₃, which behaves as a flocculant, and leads to a reduction of the chemical oxygen demand (COD).

-Table 4-

CONCLUSION

This research work reports the usage of iron (II) gluconate as a reductant in the indigo dyeing process. A brief examination of the electron donor-acceptor character and the polarizability of iron(II) gluconate and indigo was carried out using the DFT/B3LYP under 6-311 G basis set. The global reactivity descriptors proves that iron (II) gluconate molecule is a very stable with high hardness, low softness and a large energy gap. A full factorial experimental design revealed that an iron (II) gluconate concentration of $20 \text{ g}\cdot\text{L}^{-1}$, a sodium hydroxide concentration of $20 \text{ g}\cdot\text{L}^{-1}$, and a temperature of 75° C were the optimal dyeing parameters to attain maximal color strength. The evaluation of residual dyeing baths confirmed the potential of the process using iron (II) gluconate to reduce wastewater pollution. Furthermore, following the reduction process, iron (II) gluconate will be transformed into its ferric form, offering the additional benefit of being applicable as coagulants in subsequent waste treatment procedures. Finally, the dyeing process proposed in this study offers denim fabric manufacturers the opportunity to reduce the environmental impact of denim dyeing while attaining satisfactory dyeing performance at reasonable costs.

References

1. L. Xiaoyan, K. Wang, M. Wang, W. Zhang, J. Yao, S. Komarneni, J. Clean. Prod. 276 (2020) 123251. <https://doi.org/10.1016/j.jclepro.2020.123251>
2. T. M. Hsu, D.H. Welner, Z.N. Russ, B. Cervantes, R. L. Prathuri, P. D. Adams, J. E. Dueber, Nat. Chem. Biol. 24 (2018) 256–261. <https://doi.org/10.1038/nchembio.2552>
3. X.Y. Wang, S.C. Sevov, Chem. Mater. 19 (2007) 4906-4912. <https://doi.org/10.1021/cm071480x>
4. M. Abdelileh, A.P. Manian, D. Rhomberg, M. Ben Ticha, N. Meksi, N. Aguiló-Aguayo, T. Bechtold, J. Clean. Prod. 266 (2020) 121753. <https://doi.org/10.1016/j.jclepro.2020.121753>.
5. T. Bechtold, E. Burtscher, A. Turcanu, O. Bobleter, Text. Res. J. 67 (1997) 635-642. <https://doi.org/10.1177/004051759706700902>.
6. T. Bechtold, A. Turcanu, J. Appl. Electrochem. 34 (2004) 1221-1227. <https://doi.org/10.1007/s10800-004-1707-z>.
- [7] A. Turcanu, C. Fitz-Binder, T. Bechtold, J. Electroanal. Chem. 654 (2011) 29-37. <https://doi.org/10.1016/j.jelechem.2011.01.040>
8. C. Yi, X. Tan, B. Bie, H. Ma, H. Yi, Sci. Rep. 10 (2020) 4927-4928. <https://doi.org/10.1038/s41598-020-61795-5de>
9. Y. Changhai, T. Xiaodong, Z. Yang, X. Jie, Z. Hantao, L. Xueding, Z. Danying, H.Ping, Z. Jin, (Wuhan Textile University), CN201710044213.8A (2017).
10. L. Xiaoyan, W. MengQian, W. Gang, Y. Jiming, Pigm. Resin. Technol, 50 (2021) 185-193. <http://dx.doi.org/10.1108/PRT-04-2020-0035>
11. N. Meksi, M. Kechida, F. Mhenni, Chem. Eng. J. 131 (2007) 187-193. <https://doi.org/10.1016/j.cej.2007.01.001>.
12. N. Meksi, M. Ben Ticha, M. Kechida, M.F. Mhenni, Chem. Res. 49 (2010) 12333-12338. <https://doi.org/10.1021/ie100974>
13. N. Meksi, M. Ben Ticha, M. Kechida, M.F. Mhenni, J. Clean. Prod. 24 (2012) 149-158. <https://doi.org/10.1016/j.jclepro.2011.11.062>.
14. J.N. Chakraborty, R.B. Chavan, AATCC Rev. 4 (2004) 17-20. https://www.researchgate.net/publication/290277788_Dyeing_of_cotton_with_vat_dyes_using_ironII_salt_complexes
15. J.N. Chakraborty, M. Das, R.B. Chavan, Melliand Int. 12 (2005) 319-323. https://www.researchgate.net/publication/290652040_Kinetics_of_dyeing_and_properties_of_ironII_salt_complexes_for_reduction_of_vat_dyes
16. R.B. Chavan, J.N. Chakraborty, Color. Technol. 117 (2001) 88-94. <https://doi.org/10.1111/j.1478-4408.2001.tb00340.x>.

17. T. Koopmans, *Physica* 1 (1933) 104-113. [https://doi.org/10.1016/S0031-8914\(34\)90011-2](https://doi.org/10.1016/S0031-8914(34)90011-2)
18. V.C. Mudnoor, J.N. Chakraborty, *Fibers Polym.* 21 (2020) 1061-1070.
<https://doi.org/10.1007/s12221-020-9247-7>
19. J.H. Xin, C.L. Chong, T. Tu, *Color. Technol.* 116 (2000) 260-265.
<https://doi.org/10.1111/j.1478-4408.2000.tb00044.x>
20. P. Kubelka, F. Munk, *Zh. Tekh. Fiz.* 12 (1931) 593–601.
<https://www.graphics.cornell.edu/~westin/pubs/kubelka.pdf>
21. M. Ben Ticha, N. Meksi, N. Drira, M. Kechida, M.F. Mhenni, *Ind. Crops. Prod.* 46 (2013) 350-358.
<https://doi.org/10.1016/j.indcrop.2013.02.009>
22. F. Harrlekas, Doctoral thesis, Institut National Polytechnique de Lorraine (2008). <https://hal.univ-lorraine.fr/tel-01752986/document>
23. J. Rodier, C. Bazin, J. Broutin, P. Chambon, H. Champsaur, L. Rodi, *L'analyse de l'eau : Eaux naturelles eaux résiduaires eaux de mer*, Dunod, Paris (1996), p.1384. ISBN : 978-2-10-002416-2.
24. M.E.R. Carmona, M.A.P. Da Silva, S.G.F. Leite, *Process Biochem.* 40 (2005) 779–788.
<http://doi.org/10.1016/j.procbio.2004.02.024>
25. A.Y. Musa, A.H. Kadhum, A.B. Mohamad, A.A. Rahoma, H. Mesmari, *J. Mol. Struct.* 969 (2010) 233-237. <http://doi.org/10.1016/j.molstruc.2010.02.051>
26. G. Gece, S. Bilgic, *Corros. Sci.* 51 (2009) 1876-1878. <https://doi.org/10.1016/j.corsci.2009.04.003>
27. I.B. Obot, N.O. Obi-Egbedi, S.A. Umoren, *Int. J. Electrochem. Sci.* 4 (2009) 863-877.
https://www.researchgate.net/publication/261725755_Adsorption_Characteristics_and_Corrosion_Inhibitive_Properties_of_Clotrimazole_for_Aluminium_Corrosion_in_Hydrochloric_Acid
28. K. Sayin, D. Karakaş, N. Karakuş, T.A. Sayin, Z. Zaim, S.E. Kariper, *Polyhedron* 90 (2015) 139-146.
<https://doi.org/10.1016/j.poly.2015.01.047>
29. K. Fukui, *Science* 218 (1982) 747-754.
<https://www.science.org/doi/10.1126/science.218.4574.747>
30. T. Karakurt, M. Dinçer, A. Çukurovalı, I. Yılmaz, *J. Mol. Struct.* 991 (2011) 186-201.
<https://doi.org/10.1016/j.molstruc.2012.05.022>

Figure Captions

Figure 1: LUMO-HOMO energy gap at B3LYP/6-311 (level of theory) for : (a) iron (II) gluconate and (b) indigo.

Figure 2: The total electron density surface of iron (II) gluconate

Figure 3: Evolution of the redox potential RP(mV) and color strength K/S as a function of: (a) reduction temperature, (b) iron (II) gluconate concentration and (c) akali concentration. (RP and K/S values given as mean and standard deviation of three measurements).

Figure 4 : (a) Main effects plots, (b) Interaction diagrams, and (c) Contour graphs for the color strength of the indigo-dyed samples and the redox potential

Table 1: The optimized calculations of global reactivity descriptors for iron (II) gluconate and indigo at B3LYP-311G (level of theory)

| Reactivity descriptors (eV) | Iron (II) gluconate | Indigo |
|-------------------------------------|---------------------|--------|
| E_{HOMO} | -6.19 | -5.52 |
| E_{LUMO} | -1.73 | -3.21 |
| Ionization energy (IE) | 6.19 | 5.52 |
| Electron affinity (EA) | 1.73 | 3.21 |
| Electronegativity (χ) | -3.96 | - 4.37 |
| energy gap | 4.45 | 2.31 |
| Hardness (η) | 2.23 | 1.16 |
| Softness (S) | 0.224 | 0.58 |
| Chemical potential (μ) | 3.96 | 4.37 |
| Electrophilicity index (ω) | 3.52 | 8.25 |

Table 2: Optimal conditions proposed by the Box-Benken design

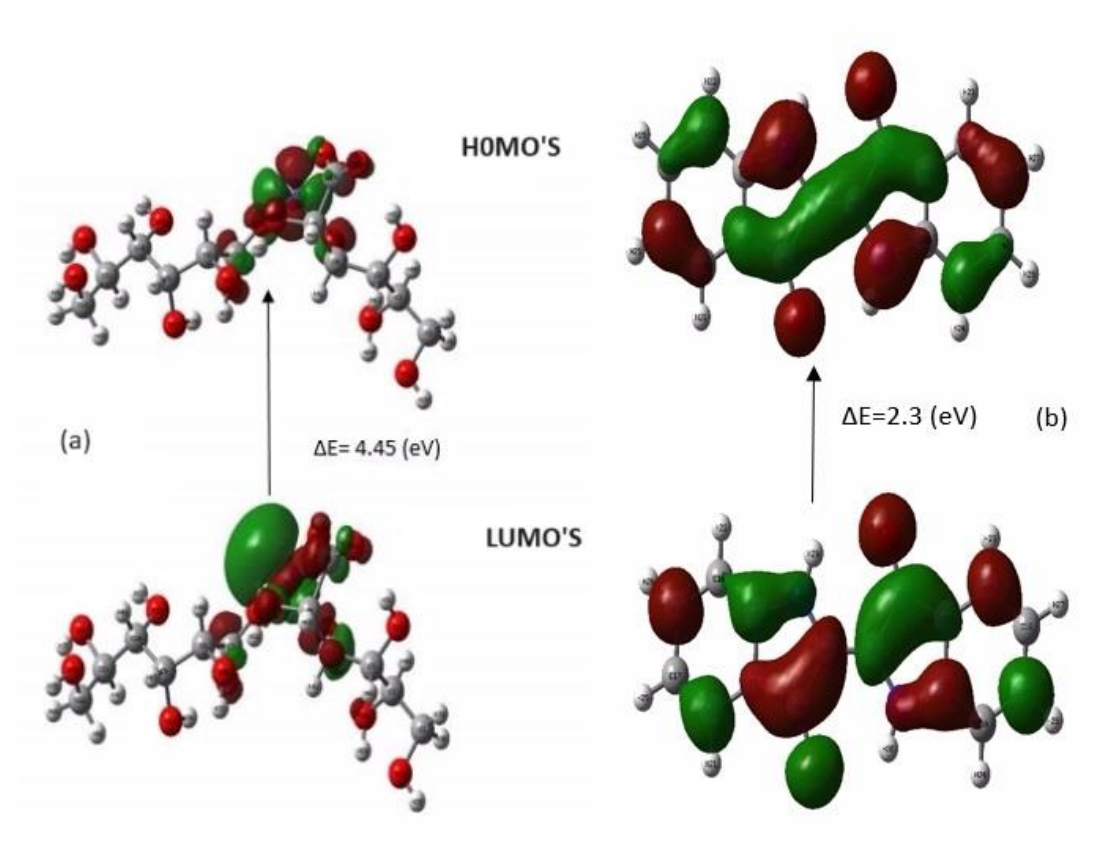
| Red(g·L⁻¹) | S (g·L⁻¹) | T(C°) | K/S (theoretical) |
|------------------------------|-----------------------------|--------------|--------------------------|
| 20 | 20 | 75 | 20 |

Table 3: Comparison of dyeing performance of the processes using sodium dithionite and iron (II) gluconate

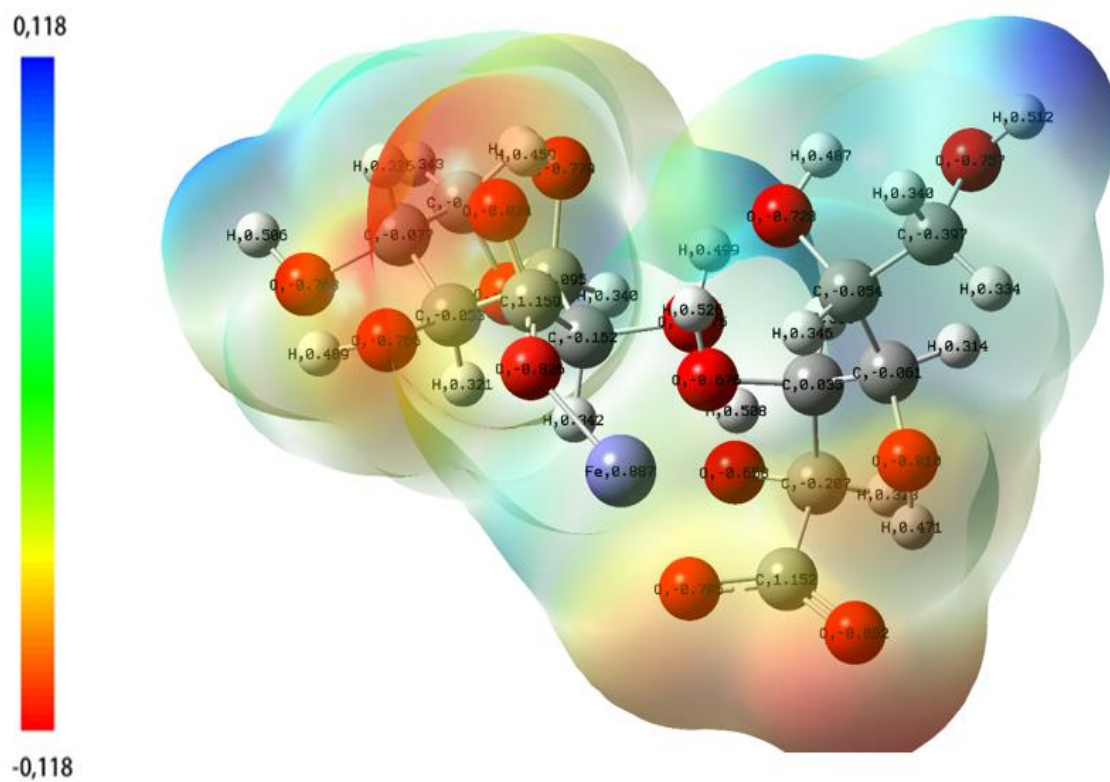
| Systems | Fastness properties | | | Light | RP(mV) | K/S | E(%) |
|----------------------------|---------------------|---------|-----|-------|--------|-----|------|
| | Washing | Rubbing | | | | | |
| | | Dry | Wet | | | | |
| <i>Iron (II) gluconate</i> | 4 | 5 | 4 | 7 | -730 | 20 | 23.7 |
| <i>Sodium dithionite</i> | 4 | 4 | 1-2 | 5 | -780 | 17 | 18 |

Table 4: Environmental evaluation of the dyeing processes

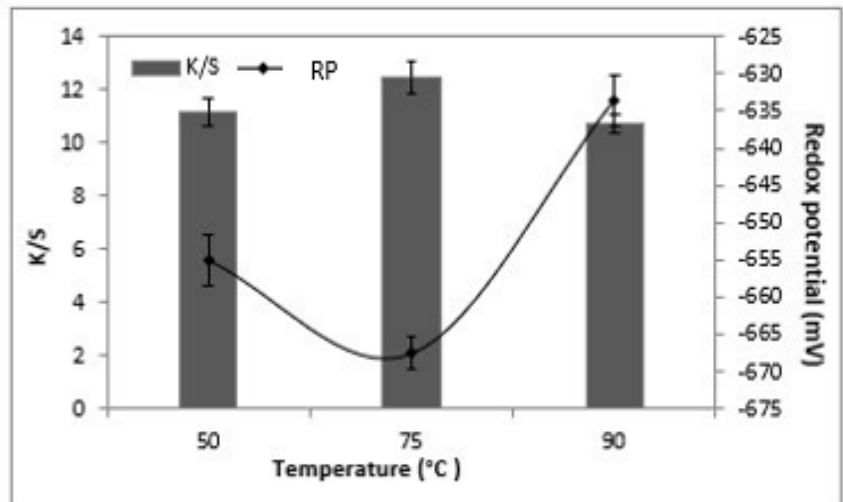
| Reducing agents | pH | COD (mgO₂.L⁻¹) | BOD₅ (mgO₂.L⁻¹) | COD/BOD₅ |
|----------------------------|-----------|---|---|----------------------------|
| <i>Sodium dithionite</i> | 12.17 | 12462 | 2036 | 6.12 |
| <i>Iron (II) Gluconate</i> | 12.23 | 5120 | 2300 | 2.22 |



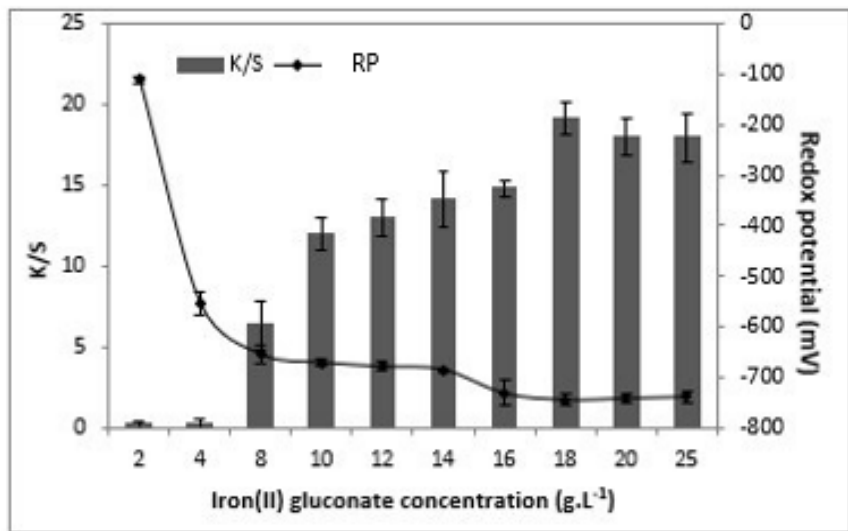
-Figure 1 -



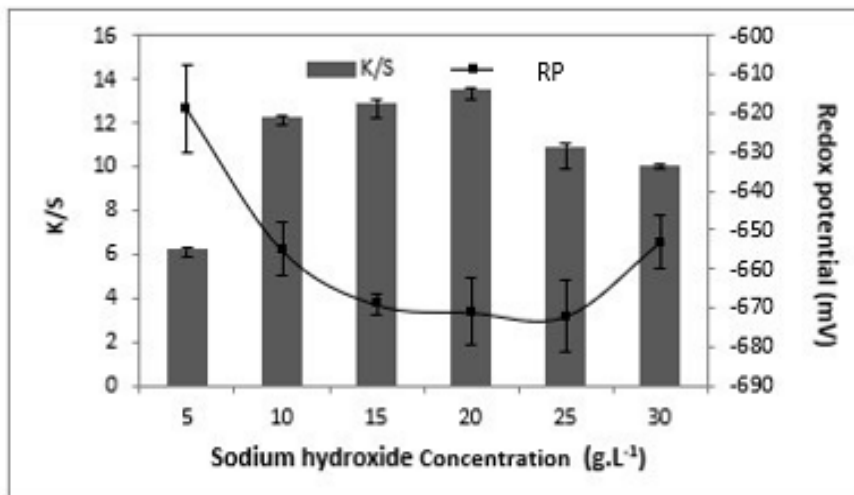
-Figure 2 -



(a)

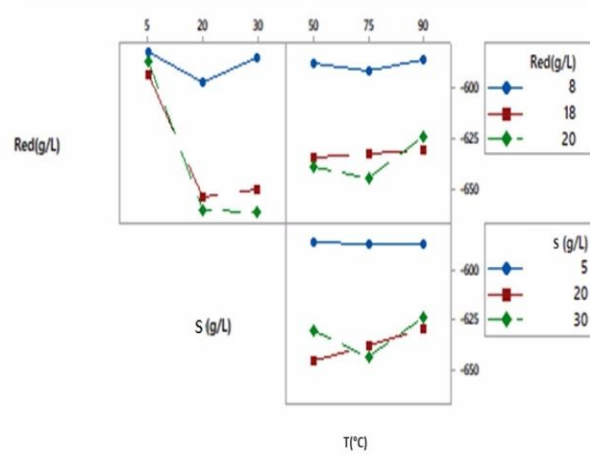
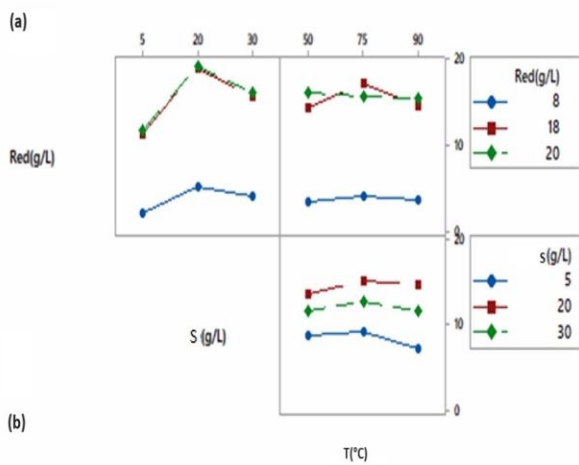
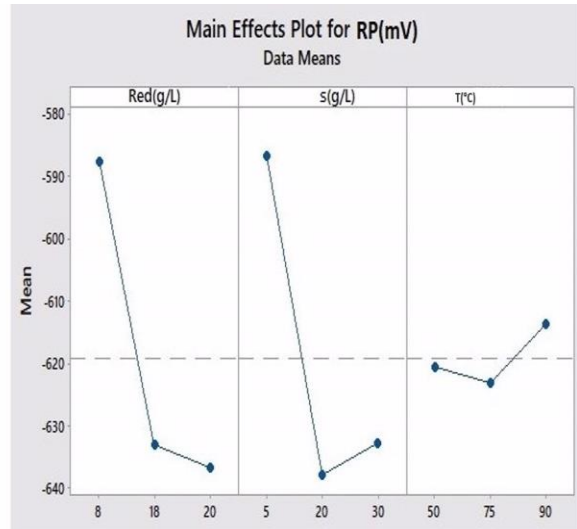
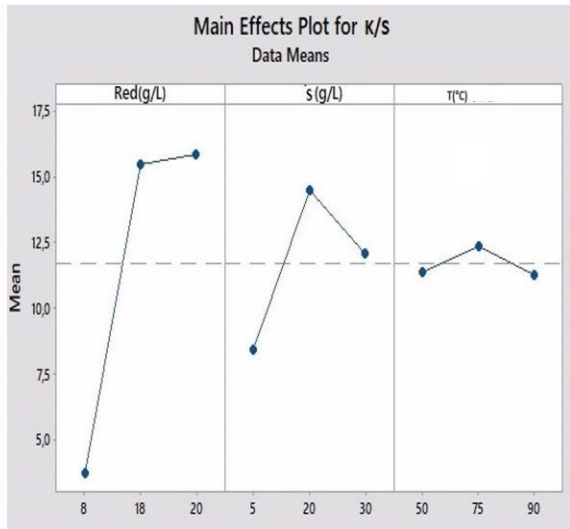


(b)

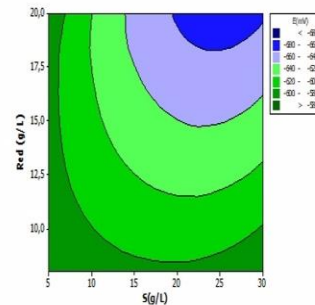
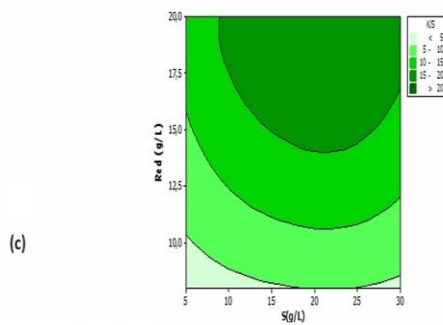
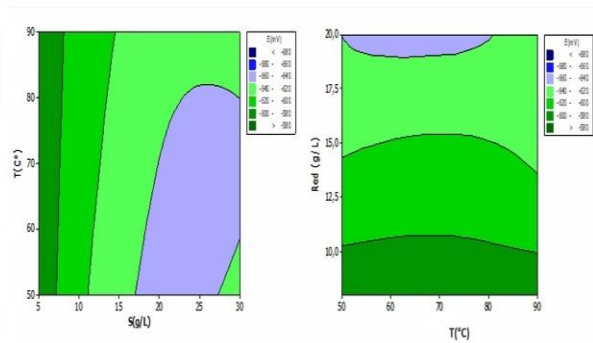
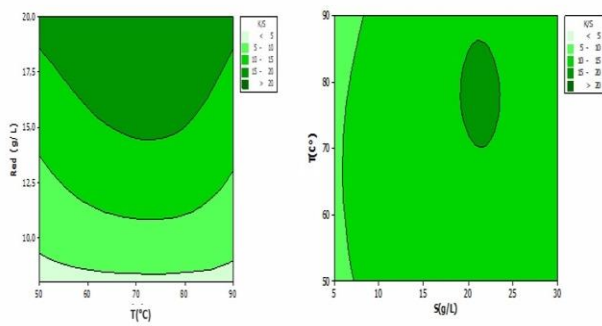


(c)

-Figure 3-



(b)



-Figure 4-